**How to cite:** Creţu, C., Ichim, P., Sfîcă, L., Breabăn, I.-G. (2022) Relationship Between Land Surface Temperature and Imperviousness Density in The Urban Area of Iasi. *2022 "Air and Water – Components of the Environment" Conference Proceedings*, Cluj-Napoca, Romania, p. 12-18, DOI: 10.24193/AWC2022_02.

# RELATIONSHIP BETWEEN LAND SURFACE TEMPERATURE AND IMPERVIOUSNESS DENSITY IN THE URBAN AREA OF IASI

***Claudiu CREȚU[1], Pavel ICHIM[1], Lucian SFÎCĂ [1], Iuliana-Gabriela BREABĂN[1]***

**DOI: 10.24193/AWC2022_02**

**ABSTRACT.** This study aims to quantify the relationship between Land Surface Temperature (LST) and Imperviousness Density (IMD) in Iaşi. This was done through linear regression analysis which involves quantifying the relationship between one independent variable (explanatory, predictor) and one dependent variable (response). Thus, in our study, the dependent variable is represented by the LST product obtained through MODIS sensors in the period 2014-2018, while the independent variable is represented by IMD. The coefficient of determination ($R^2$) obtained, higher than 0.5 for most of the year, indicates a statistically significant relationship between LST and IMD. The highest values of $R^2$ are identified during the day spring and summer seasons. Thus, 70% and respectively 80% of the spatial variation of LST is explained by the distribution of IMD during these two seasons and the regression coefficients indicate, on the one hand, that the relationship between the two variables is a direct one (LST values increase at the same time with IMD values), and on the other hand, that the increase of LST corresponds to a gradient between 0.3-0.6$^o$C per 10% IMD. During the day, the lowest values of $R^2$ appear in autumn and winter seasons, as a result of the local topography that facilitates the frequency of thermal inversions in this period of the year. On the other hand, during the night, $R^2$ has values between 0.40 and 0.60, with the lowest values in the autumn season and the highest in the spring season, respectively.

**Keywords**: land surface temperature (LST), imperviousness density (IMD), MODIS, linear regression, Iasi city.

## 1. INTRODUCTION

Land surface temperature (LST) is a key parameter in the physics of land surface processes on regional and global scales (Morillas, 2013) and is usually estimated by instruments that are mounted on a satellite platform (Pichierri, 1982; Streuker, 2002; Voogt, 2003; Hung, 2006; Li, 2018; Zhou, 2019). Those observations have the advantage that they can provide a spatially continuous image of LST across a city and helps overcome difficulties associated with using in situ sensors to sample adequately the vast range of surface facets comprising an urban system (Oke, 2017).

The sensors placed on board of the satellites are passive and therefore receive and measure both the reflected shortwave radiation (non-thermal spectral bands) and the

[1] Faculty of Geography and Geology, Alexandru Ioan Cuza University of Iaşi. (sfical@yahoo.com)

longwave radiation emitted (thermal bands) by the Earth's surface and atmosphere (Mohamed et al, 2017).

These sensors are an important source of data for studying Surface Urban Heat Island (SUHI). To study SUHI, Moderate Resolution Imaging Spectroradiometer (MODIS) is a valuable data source due to its high temporal resolution, average spatial resolution (about 1 km), global coverage and free data availability (Hung, 2006; Cheval, 2009; Anniballe, 2014; Cheval, 2015; Crețu, 2020, Cheval 2021). LST is highly be influenced by surface properties. Five properties exert strong control on surface temperatures. These refer to the geometric properties (slope angle, azimuth), radiative properties (reflect shortwave and longwave radiation and emit longwave radiation), thermal properties of the material, moisture properties (surface and near-surface) or aerodynamic properties of the surface (Oke et al, 2017).

## 2. STUDY AREA, DATA AND METHODS

Iași city is a medium-size city with a population of almost 335.000 inhabitants in 2012 (Roşu, 2015) located in the northeastern part of Romania in the historical province of Moldova, at a mean altitude of 87 m above sea level (Fig. 1).

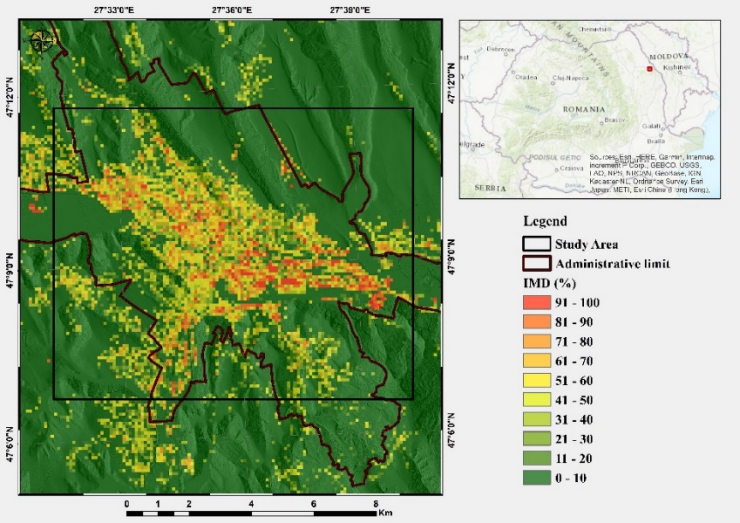


*Figure 1 Physico-Geographical position and IMD of the studied area*

The MOD11A1 V6 and MYD11A1 V6 products registered by MODIS between 2014-2018 were used for this study. The daily LST product at 1km spatial resolution is a tile of daily LST product gridded in the Sinusoidal projection. A tile contains 1200 x 1200 grids in 1200 rows and 1200 columns. The exact grid size at 1km spatial resolution is 0.928km by 0.928km. More details about these products are presented in detail in the Collection-6 MODIS Land Surface Temperature Products User Guide (Wan, 1996; Wang, 2012; Wan, 2014).

The products needed for this study were obtained through "The Application for Extracting and Exploring Analysis Ready Samples" (AρρEEARS) for an area of approximately 100 $km^2$ and processed through Qgis 3.18.1.

The process involved the use of images with at least 92.0 % valid pixels within the studied area, the remaining 8.0 % being covered by clouds. This was done using the r.fillnulls function that covers data gaps by applying spline interpolation, the bilinear method (the number of selected images is shown in Table 1). Also using the bilinear method, in order to improve the spatial resolution of the LST data, a resampling of them was performed, thus bringing them to a resolution of 100x100m. The last step involved obtaining weighted averages for observations during the day and nighttime and multiannual seasonal averages.

*Table 1 Satellite overpass and number of images used for each MODIS product (2014-2018)*

| Modis Product | MAM | JJA | SON | DJF | Total |
|---|---|---|---|---|---|
| MOD11A1-Daytime | 211 | 301 | 180 | 65 | 757 |
| MOD11A1-Nighttime | 183 | 147 | 161 | 119 | 610 |
| MYD11A1-Daytime | 185 | 255 | 160 | 42 | 642 |
| MYD11A1-Nighttime | 225 | 241 | 180 | 102 | 748 |
| Total | 804 | 944 | 681 | 328 | 2757 |

Urban development of a previously rural sites leads to significant disturbance of the surface geometry and properties. Natural materials are removed, replaced or modified by a new mix introduced that is often dominated by construction materials. The radiative, aerodynamic, thermal and moisture properties of these materials are radically different to natural ones leading to a modified surface. These materials modify the Surface Energy Balance (SEB) and, thus, the spatial pattern of LST (Chandler, 1960; Arnfield, 2003; Oke, 2017; Deilami, 2018).

To show the relationship between artificial impervious cover and LST we used Imperviousness Density (IMD). The imperviousness products capture the percentage and change of soil sealing. Sealed/Impervious areas are characterized by the substitution of the original (semi-) natural land cover or water surface with an artificial, often impervious cover. The imperviousness captures the spatial distribution of artificially sealed areas, including the level of sealing of the soil per area unit. The level of sealed soil (imperviousness degree 1-100%) is produced using a semi-automated classification, based on calibrated NDVI (Copernicus Land Monitoring Service).

## 3. RESULTS AND DISCUSSIONS

The spatial pattern of LST is the outcome of the SEB of urban facets, canyons and neighborhoods, and they are subject to the controls exerted by the surface properties and structure. The SEB is the fundamental starting point if we want to

understand and predict surface microclimates and climates of the atmospheric boundary layer (ABL) (Oke, 2017).

The city is comprised extensively of impermeable manufactured materials (Figure 1) and the canyon formed by the buildings and road regulates aerodynamic and radiative exchanges with the overlying atmosphere.

Urban area presents an increased imperviousness density with values between 50 and 100%, while the neighboring areas have lower values, between 0-50%. The link between IMD and LST values is shown in Figure 2 by linear regression.

The resulting equation is of the form $y = ax + b$, where $y$ is LST, $b$ is the free term, indicating the value of LST when $x = 0$, and $a$ is the regression coefficient, having gradient significance (how much LST changes when changing IMD by one unit).

The coefficient of determination ($R^2$) indicate the share of the dependent variable (LST) estimated by the explanatory variable (x) by the respective regression equation. $R^2$ values, all higher than 0.40, indicate clearly a statistically significant relationship between LST and IMD regardless of the seasons. The highest values of $R^2$ are identified during the day in both the spring and summer seasons. Thus, 70% (Figure 2, A) and respectively 80% (Figure 2, C) of the spatial variation of LST is explained by the distribution of IMD during these two seasons and the regression coefficients indicate, on the one hand, that the relationship between the two variables is a direct one (LST values increase in the same time with IMD values), and on the other hand, that the increase of LST takes place after a gradient with the value of 0.3 respectively $0.6^{o}C/10\%$. During the day, the lowest values of $R^2$ appear in autumn (Figure 2, E) and winter seasons Figure 2, G), as a result of the local topography that facilitates the frequency of thermal inversions in this period of the year.

On the other hand, during the night (Figure 2, B-D-F-H), $R^2$ has values between 0.40 and 0.60, with the lowest values in the autumn season and the highest in the spring season, respectively.

The relationship between the two variables can be explained by the fact that the LST of urban area as observed from satellites has higher values in the daytime and during summer (Ho, 2014), but in all seasons the nocturnal LST is smaller than during daytime and it exhibits less spatial variability (Imhoff et al., 2010, Peng et al., 2011). Seasonal variation of LST of urban area depends on changes in surface properties, especially soil moisture. Wet winters are typical of many mid-latitude cities, and this drives to increases soil moisture and creates relatively large soil thermal admittance, that in turn reduces nocturnal surface cooling resulting in smaller values of LST (Oke, 2017).

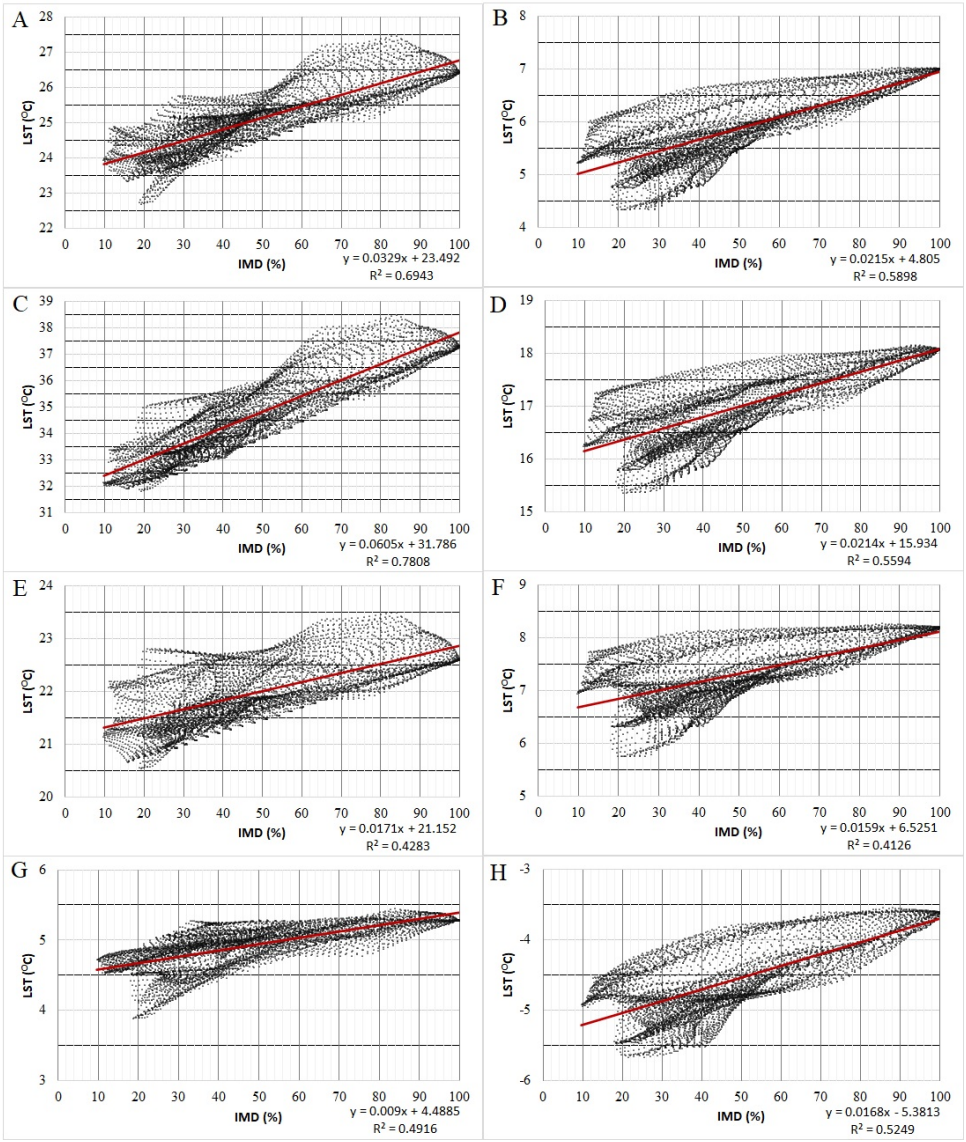


*Figure 2 Linear regression between IMD and LST. Spring mean LST *Day (A), Spring mean LST *Night (B), Summer mean LST *Day (C), Summer mean LST *Night(D), Autumn mean LST *Day (E), Autumn mean LST *Night (F), Winter mean LST *Day (G), Winter mean LST *Night (H).*

## 4. CONCLUSIONS

The LST has a complex variability mainly due to the geometry, radiative and thermal properties of surface. The materials used to construct cities are extremely varied (e.g. concrete, asphalt, stone, brick, wood, metal, glass, tile) leading to changes in natural surfaces (e.g. soils, vegetation, water). Each material has its own

distinct mix of radiative, roughness, thermal and moisture properties. Thus, with the increase of artificial surfaces, the LST values also increase.

The highest LST values are recorded during the day, in the spring and summer seasons, respectively. At the same time, the highest values of $R^2$ appear during this period, indicating a strong relationship between LST and IMD.

In the future we intend to use this data for a complex assessment of the surface heat island and to investigate its relation with the land cover, but also the relationship between SUHI and air urban heat island.

## REFERENCES


1. Anniballe, R.; Bonafoni, S.; Pichierri, M. Spatial and temporal trends of the surface and air heat island over Milan using MODIS data. *Remote Sens. Environ*. **2014**, 150, 163–171.
2. Arnfield J (2003) Two decades of urban climate research: a review of turbulence, exchanges of energy and water, and the urban heat island. *Int J Climatol* 23(1):1–26. https://doi.org/10.1002/joc.859
3. Chandler TJ (1960) Wind as a factor of urban temperatures: a survey in north-east London. *Weather* 15:204–213.https://doi.org/10.1002/j.1477-8696.1960. tb00659.x
4. Cheval, S., Dumitrescu, A. (2009) The July urban heat island of Bucharest as derived from modis images. *Theor Appl Climatol* 96, 145–153. https://doi.org/10.1007/s00704-008-0019-3
5. Cheval, S., Dumitrescu, A. (2015) The summer surface urban heat island of Bucharest (Romania) retrieved from MODIS images. *Theor Appl Climatol* **121,** 631–640.
6. Cheval, S., Dumitrescu, A., & Bell, A. (2009). The urban heat island of Bucharest during the extreme high temperatures of July 2007. *Theoretical and Applied Climatology, 97(3-4), 391–401.* doi:10.1007/s00704-008-0088-3
7. Cheval, S., Dumitrescu, A., Irașoc, A., Paraschiv, M.G., Perry, M., Ghent, D. (2014) MODIS-based climatology of the Surface Urban Heat Island at country scale (Romania). *2021 41 101056 https://doi.org/10.1016/j.uclim.2021.101056 Clim. Res*. 59, 1–13.
8. Creţu,Ş.-C.; Ichim, P., Sfîcă, L. (2020) Summer urban heat island of Galat,i city (Romania) detected using satellite products. *PESD* 2020, 4, 272.
9. Deilami, K., Kamruzzaman, M., Liu, Y. (2018) Urban heat island effect: A systematic review of spatio-temporal factors, data, methods, and mitigation measures. *Int. J. Appl. Earth Obs. Geoinf.* 67, 30–42.
10. Ho, H.C., Knudby, A., Sirovyak, P., Xu, Y., Hodul, M. (2014) Henderson, S.B. Mapping maximum urban air temperature on hot summer days. *Remote Sens. Environ.* 154, 38–45.
11. Hung, T., Uchihama, D., Ochi, S., Yasuoka, Y. (2006) Assessment with satellite data of the urban heat island effects in Asian mega cities. *Int. J. Appl. Earth Obs. Geoinf.* 8, 34–48.
12. Imhoff, M.L.; Zhang, P.; Wolfe, R.E.; Bounoua, L. (2010) Remote sensing of the urban heat island effect across biomes in the continental USA. *Remote Sens. Environ.,* 114, 504–513.

13. Li, H.; Zhou, Y.; Li, X.; Meng, L.; Wang, X.; Wu, S.; Sodoudi, S. (2018) A new method to quantify surface urban heat island intensity. *Sci. Total Environ*., 624, 262–272.
14. Mohamed, A.A.; Odindi, J.; Mutanga, O. (2017) Land surface temperature and emissivity estimation for urban heat island assessment using medium- and low-resolution space-borne sensors: A review. *Geocarto Int.*, 32, 455–470.
15. Oke, T.R. (1982) The energetic basis of the urban heat island. *Q. J. R. Meteorol. Soc.*, 108, 1–24.
16. Peng, S., Piao, S., Ciais, P., Friedlingstein, P., Ottle, C., Breon, F.-M., Nan, H., Zhou, L., Myneni, R.B. (2012) Surface urban heat island across 419 global big cities. *Environ. Sci. Technol.,* 46, 696–703.
17. Pichierri, M., Bonafoni, S., Biondi, R. (2012) Satellite air temperature estimation for monitoring the canopy layer heat island of Milan. *Remote Sens. Environ*., 127, 130–138.
18. Roşu L, Blăgeanu A (2015) Evaluating performances of a public transport network in a post-socialist city using quantitative spatial approach. *Urbani Izziv* 26(2):103–116. https://doi.org/10.5379/ urbani-izziv-en-2015-26-02-002
19. Streutker, D.R. (2002) A remote sensing study of the urban heat island of Houston, Texas. *Int. J. Remote Sens.,* 23, 2595–2608.
20. Streutker, D.R. (2003) Satellite-measured growth of the urban heat island of Houston, Texas. *Remote Sens. Environ.,* 85, 282–289.
21. Voogt, J.A.; Oke, T.R. (2003) Thermal remote sensing of urban climates. *Remote Sens. Environ.,* 86, 370–384.
22. Wan, Z.; Dozier, J. A. (1996) generalized split-window algorithm for retrieving land-surface temperature from space.IEEE Trans. *Geosci. Remote. Sens*., 34, 892–905.
23. Wan, Z. (2014) New refinements and validation of the Collection-6 MODIS land-surface temperature/emissivity product. *Remote Sens. Environ*., 140, 36–45.
24. Wang, Z. (2012) Collection-6 MODIS Land Surface Temperature Products Users' Guide warming trend. *Carpathian J. Earth Environ. Sci.*, 7, 97–106.
25. Weng, Q.; Larson, R.C. (2005) Satellite remote sensing of urban heat islands: Current practice and prospects. In *Geo-Spatial Technologies in Urban Environments*; Jensen, R.R., Gatrell, J.D., McLean, D.D., Eds.; Springer: Berlin/Heidelberg, Germany, pp. 91–111.
26. Wan, Z., Hook, S., Hulley, G. (2015). *MYD11A1 MODIS/Aqua Land Surface Temperature/Emissivity Daily L3 Global 1km SIN Grid V006*. NASA EOSDIS Land Processes DAAC. Accessed 2021-03-22 frOM https://doi.org/10.5067/MODIS/MYD11A1.006. Accessed March 22, 2021.
27. Zhou, D., Xiao, J., Bonafoni, S., Berger, C., Deilami, K., Zhou, Y., Frolking, S., Yao, R., Qiao, Z., Sobrino, J.A. (2019) Satellite Remote Sensing of Surface Urban Heat Islands: Progress, Challenges, and Perspectives. *Remote Sens.*, *11*, 48. https://doi.org/10.3390/rs11010048
28. *** *Climate of Romania*, 2008, Editura Academiei Române.
29. *** ”AppEEARS Team. (YYYY). *Application for Extracting and Exploring Analysis Ready Samples (*AppEEARS). Ver. X.X. NASA EOSDIS Land Processes Distributed Active Archive Center (LP DAAC), USGS/Earth Resources Observation and Science (EROS) Center, Sioux Falls, South Dakota, USA. Accessed Month, DD, YYYY. https://lpdaacsvc.cr.usgs.gov/appeears/”